

## CRUSTAL THICKNESS VARIATIONS IN THE SOUTHEASTERN MEDITERRANEAN REGION, INCLUDING NORTHEASTERN PART OF EGYPT, AS DEDUCED FROM 3D GRAVITY MODELING

S. Saleh

National Research Institute of Astronomy and Geophysics (NRIAG), 11421,  
Helwan, Cairo, Egypt, E-mail: salahsmm@yahoo.com

### تغيرات سماكة القشرة الأرضية في منطقة جنوب شرق البحر الأبيض المتوسط، بما في ذلك الجزء الشمالي الشرقي من مصر، والمستنتجة من البيانات التثاقلية ثلاثية الأبعاد

**الخلاصة:** تم تحديد سماكة القشرة الأرضية تتأقليا من المنطقة الجنوبية الشرقية لمنطقة حوض البحر الأبيض المتوسط، والتي تمتد جنوبا من جزء قبالة الساحل الشمالي الشرقي من مصر (شمال سيناء) إلى الجزء الجنوبي من قبرص شمالا، وذلك باستخدام تحليل بيانات البوجير ثلاثية الأبعاد. وقد حسنت البيانات شكل وتوزيع الكثافات على البروفيلات التثاقلية ثلاثية الأبعاد. كانت الحدود المحيطية-القارية وقعت بعد الحد الشمالي للقارة الأفريقية، وتم تعريف شكل تضاريس صخور القاعدة (سماكة قطاع الصخور الرسوبية)، وخرائط عمق الموهو. كما تم تقييم خرائط البوجير لكلا من الشاذات المحلية والإقليمية لإظهار المزيد من الصور التفصيلية للتراكيب العميقة والضحلة.

وبشكل عام، يعتبر هذا المجال الإقليمي في منطقة تحت الدراسة يتأثر بشكل رئيسي من تباين أختلافات الكثافة بين القشرة والوشاح العلوي. ففي الجزء الشمالي من مصر، نجد أن الشاذات الإقليمية تزداد من -30 إلى +40 ملي جال. وهذا يشير إلى أن سماكة القشرة الأرضية تتخفص نحو البحر الأبيض المتوسط. أما الشاذات السالبة للتثاقلية المحلية (المتبقية) لها قيم حد ادني تتراوح بين -30 و -25 ملي جال في دلتا النيل والحوض الشامي على التوالي، وذلك بسبب ارتباطهم مع أعطية الرسوبية السمكة، فضلا عن حالات الشاذات التثاقلية المحلية السالبة والتي لها قيم -30 ملي جال حول جنوب قبرص ترتبط بتراكيب التتابع الرسوبي و شكل تضاريس صخور القاعدة.

وتظهر النتائج أيضا وقوع أجزاء القشرة القارية السمكة ذات سمك حوالي 21 كلم في شمال مصر، وعلى الأقل في بعض المناطق في شمال سيناء، التي تغطيها رواسب رسوبية رقيقة. وعلى بعد كيلومترات قليلة شمالا، وخاصة أسفل أجزاء من المناطق الساحلية، سمك القشرة يقل بشكل مفاجئ (المنطقة تمر بمرحلة انتقالية). وقد تبين من الدراسة وجود علاقة متبادلة عكسية بين كثافة الرسوبيات وسماكة القشرة الأرضية. وعلاوة على ذلك، لدينا نموذج يكشف عن وجود منطقة القشرة القارية تحت كتلة إراتوستينيس الجبال البحرية، مما يشير إلى تصادم وقع بين اللوحان الأفريقي والأوراسيوي. بالإضافة إلى ذلك، هذه الكتلة القارية هي في طور الخمود بنشاط، وكسر المتابعة ويجري دفعه على حد سواء تحت جزيرة قبرص في الشمال والحوض الشامي في الجنوب. في حين نجد أن نوع القشرة الأرضية تحت الحوض الشامي هو عادة محيطي، وهو مغطى بتتابع الصخور الرسوبية والتي لها سماكة أكبر من 14 كيلومترا. التثاقلية العالية لقبرص، وبالقرب من منطقة الاندساس القص، ربما نجمت عن مجموعات متباينة من صخور الافيولايت وقلّة سماكة الصخور الرسوبية، كما تم استنتاجة من النمذجة ثلاثية الأبعاد. خريطة الموهو المستنتجة خلال هذه الدراسة تبين أن عمق الموهو يتراوح من 28-30 كم تحت قبرص وتتراوح من 26-28 كم تحت جنوب ارتفاع فلورنسا إلى الجزء الشمال الغربي. ومع ذلك، فإن موهو يكمن في عمق ضحل ثابت من 22 إلى 24 كيلومترا تحت الحوض الشامي، الذي يشير إلى رفاقة سمك القشرة الأرضية تحت هذه المنطقة. وأخيرا، فإن خريطة موهو يكشف أيضا أقصى عمق لها حوالي 33-35 كم تحت شمال مصر وشمال سيناء، ذات قشرة قارية على حد سواء.

**ABSTRACT:** Crustal thickness of the Southeastern Mediterranean Basin region, which extends from the off-shore northeastern part of Egypt (northern Sinai) to the southern part of Cyprus, was gravimetrically determined, using the 3D Bouguer data analysis. The gravity data have improved both the mass geometry and the density distribution in the 3-D calculated gravity profiles. The oceanic-continental boundary occurred beyond the North African continental margin, the basement relief (sedimentary section thickness) and the Moho depth maps were defined. The regional and residual Bouguer anomaly maps were also evaluated to show more detailed pictures for the deep and shallow structures.

Generally, the regional field in the area under study is considered to be mainly influenced by the density contrast variations between the crust and the upper mantle. In the northern part of Egypt, the regional anomaly shows an increase from -30 to +40 mGal. This indicates that, the crustal thickness decreases towards the Mediterranean Sea. The residual negative anomalies with minimum values of -30 and -25 mGal in the Nile Delta and the Levantine Basin respectively, are due to their association with thick sedimentary covers, as well as the negative anomalies of -35 mGal around Southern Cyprus are related to the structures of the sedimentary sequences and the related basement relief geometry.

The results also show the occurrence of thick continental crustal parts with a thickness of approximately 21 km in Northern Egypt and at least in some areas of Northern Sinai, covered by thin sediments. A few kilometers farther to the

north, especially below the coastal parts regions, the thickness of crust decreases abruptly (transition zone). An inverse correlation between the sediment densities and the crustal thicknesses has been shown up from the study. Furthermore, our model reveals the existence of continental crustal zone below the Eratosthenes Seamount block, indicating a collision taken place between the African and Eurasian plates. Additionally, this block is in the process of actively subsiding, breaking-up and being thrust beneath both Cyprus Island to the north and the Levantine Basin to the south. Whereas, the crustal type beneath the Levantine Basin is typically oceanic, this is covered by sedimentary sequences of more than 14 km thick.

The gravity high of Cyprus, near the shear subduction zone, is possibly caused by varying combinations of ophiolites and thinning of sediments, as derived from the 3-D gravity modeling. The modeled Moho map shows a depth of 28-30 km below Cyprus and of 26-28 km beneath South Florence Rise to the northwest. However, the Moho lies at a constant shallow depth of 22 to 24 km below the Levantine Basin, which indicates thinning of the crust beneath this region. Finally, the Moho map reveals also a maximum depth of about 33-35 km beneath both Northern Egypt and Northern Sinai, with continental crust.

*Keyword: 3-D gravity modeling, Bouguer Map, Southeastern Mediterranean, Northern Egypt.*

## 1. INTRODUCTION

The Eastern Mediterranean is a tectonically complex region located in the midst of the progressive Afro-Eurasian collision. Its geological-geophysical structure has been studied for years, but it is still not completely known. The present tectonics are driven through the collision between the African and Eurasian plates, the Arabian-Eurasian convergence and the displacement of the Anatolian Aegean microplate. The boundary between the African and the Anatolian-Aegean microplates is delineated by the Hellenic arc, the Pliny Strabo trench, the Florence Rise and Cyprus in the west, while in the east the boundary has been identified in the Herodotus basin, or east of Cyprus (Aksu et al., 2005 and references therein).

Since the initiation of the plate tectonic theory, many geophysical and tectonic studies of the Eastern Mediterranean have been conducted in recent years (e.g. Woodside, 1977; Makris et al., 1983; Ben-Avraham, 1989; Ben-Avraham et al., 1987, 2002 & 2006.; Kastens, 1991; Smith et al., 1994; Garfunkel, 1998; Di Luccio and Pasyanos, 2007, Segev and Rybakov 2010 and Lev Eppelbaum and Youri Katz, 2011).

The determination of crustal thickness has been the purpose of many published works, in which a variety of geophysical techniques have been applied. Recent receiver function, surface wave and tomographic studies (for example: Ben Avraham et al., 2002; Marone et al., 2003; van der Meijde et al., 2003; Hofstetter & Bock, 2004; Koulakov et al., 2005; Makris & Yegorova, 2005) have derived the Moho depth, and mapped shear wave velocities in different sites in the Eastern Mediterranean region.

Here, we wish to provide a more local perspective on parameters such as density values in order to estimate both the crustal type and thickness variations. Crustal types beneath the Eastern Mediterranean vary from oceanic to continental and the thicknesses of sediments plays an important role in determining the nature of the crust. For example, the nature of the crust in the Levantine basin, south of Cyprus and west of the Israel and Lebanon margins, has been defined as oceanic (Khair & Tsokas, 1999) or continental (Ben Avraham et al., 2002). In the first case, the Levantine basin was formed by rifting of the African continental

crust fragments, whereas in the latter case, a sediment layer of 14-15 km overlies a thinned Precambrian continental crust. In a recent study, Ritzmann et al. (2007) found a strong negative correlation between the sediment thickness and the thickness of crystalline crust in the extensional tectonic regime of the Barents Sea. Where the crust has been extended (thin crust), there was a correspondingly thick sediment profile.

The study area has remarkably prominent sub-morphogeologic features; such as the Eastern Mediterranean Ridge, Levantine Basin, Eratosthenes Seamount, Nile cone, Northern Sinai Peninsula and Southern Cyprus. The area under investigation covers the northeastern margin of the African plate between Latitudes 30° & 35° N and Longitudes 30° & 35° E (Figure 1). The region of study is considered to be a tectonically complicated area, due to its location within the contact zone among the African, Sinai and Eurasian plates.

In the present work, an attempt is made to perform a 3-dimensional gravity modeling of the Southeastern Mediterranean and the Northern Egyptian continental margin for estimating the variations of crustal thickness beneath these regions. Basically, the previous deep seismic sounding results (Makris et al., 1983; Vidal et al., 2000 & Ben-Avraham et al., 2002 & 2006) have been used to constrain the initial density model of the 3-D gravity model planes (see the locations of seismic profiles in Fig. 2). The obtained results are supposed to fill the gaps among the northeastern continental margin of Egypt (including the Nile Delta and Northern Sinai coastal zones), Levantine basin, Eratosthenes seamount and the southern part of Cyprus. This study adds also new information about the nature of the deep structures of this region (oceanic or continental).

## 2. Geologic and Tectonic Settings

The Eastern Mediterranean region has had a complex tectonic history, since the Early Mesozoic breakup of Gondwana. Between the major plates of Africa and Eurasia, there is > 1,500-km-wide

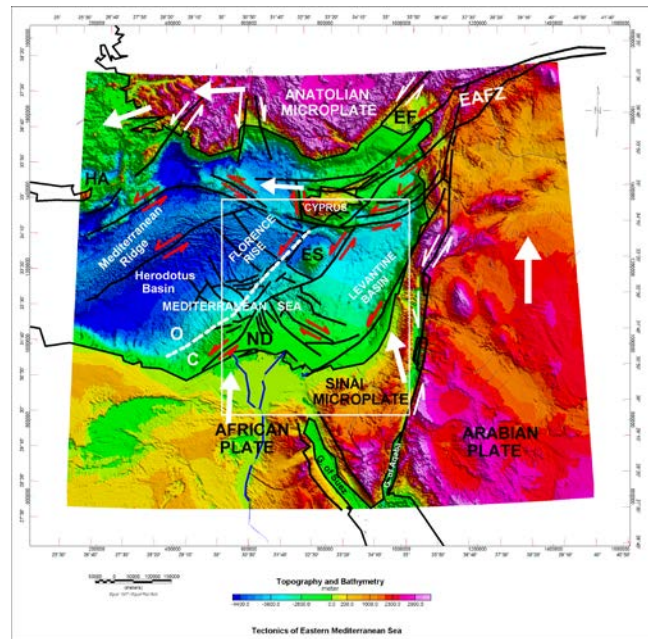


Figure (1): Present-day tectonic map of the Eastern Mediterranean region (after Harrison and Panayides (2004) and Harrison et al., (2004). ES- Eratosthenes Seamount, FR- Florence Rise, which occurs along left-lateral strike-slip structure (ten Veen et al., 2004); EF- Ecemis fault, EAFZ –Eastern Anatolian fault zone (paleo-location to the south during Mesozoic & Paleogene shown by ghost lettering) DST- Dead Sea transform, ND- Nile Delta, HA- Hellenic arc; bold dashed line is approximate boundary between oceanic (O) and continental (C) crust (Dolson et al., 2004 a and Dolson et al., 2004 b); large arrows represent relative plate motions (after Jackson and McKenzie, (1988) and McClusky et al., (2000)). The fault system between Cyprus and ES is the Cypriot transform, which marks the northern African plate boundary (Dewey et al., (1973) and Şengör et al., (1985)

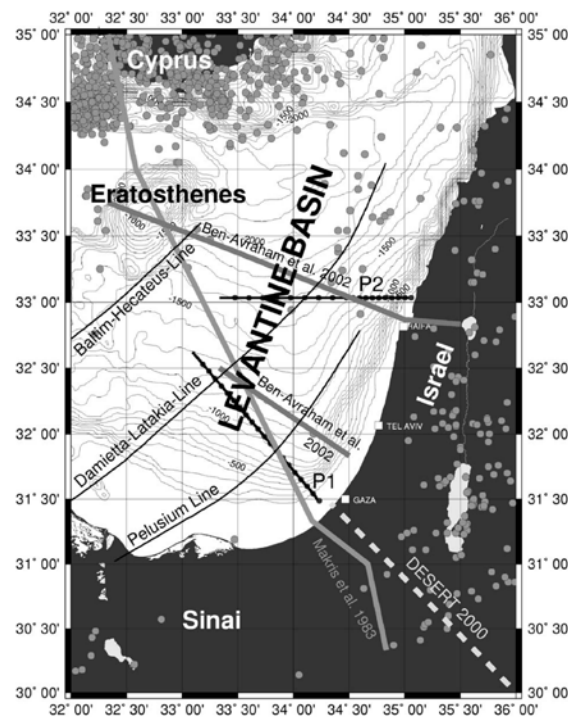


Figure (2): Map of the Levantine Basin (after Netzeband et al., 2006). Thick solid lines mark the locations of profiles P1 and P2, with solid black circles indicating the positions of the OBH. The shear zones Pelusium Line, Damietta–Latakia Line, and Baltim–Hecateus Line are shown after Neev et al. (1976). Gray circles mark hypocenters of earthquakes since 1973 according to the US Geological Survey. Previous refraction seismic lines in the Levantine Basin are marked as light gray lines.

intervening collage of differing tectonic terranes, that are the product of shearing, rifting, subduction, obduction and contraction over the past 200 Ma. The dynamics of the plate interactions are recorded in the assembly of this collage (Harrison, 2008).

There is a general agreement that, plate convergence takes place in this area (McKenzie, 1970; Smith, 1971; Ryan et al., 1971; Dewey et al., 1973; Nur & Ben-Avraham, 1978; Dercourt et al., 1986; Kempler & Ben-Avraham, 1987; Robertson, 1992; Kempler, 1994; Kempler and Garfunkel, 1995; Kempler, 1998 and others).

The formation of the Eastern Mediterranean tectonics is largely dominated by the relative movement of the Arabo-African plates and the Eurasian plate (Dewey et al., 1973). These two large blocks have converged, since the end of the Cretaceous to close the northern arm of the Tethys Ocean and form the Alpine chain between them (Biju-Duval et al., 1978).

The Eastern Mediterranean and the Levantine Basin within it are relics of the Mesozoic Neo-Tethys Ocean (Robertson and Dixon, 1984; Stampfli and Borel, 2002; and Garfunkel, 2004). The Levantine Basin (Fig. 2) is confined by the Israeli and the Egyptian coasts, Cyprus and the Eratosthenes Seamount (Figs. 1 and 2). It filled by up to 10 km of Mesozoic to Recent sediments, next to the Alpine deformation front of the Cyprian Arc, near the junction between Africa and Arabia. Away from the deformation front, the basin has undergone little deformation for the past 100 Ma, as evidenced by the deep seismic reflection profiles (Vidal et al., 2000).

Cyprus is located on the southern margin of the Anatolian microplate (Fig. 1), adjacent to the African plate boundary (Dewey et al., 1973). Because of the northward-directed movement of Africa, the Levant oceanic segment is subducted beneath the Tauric arc, south of Cyprus. The Cyprian and Hellenic arcs are dominated by compression, whereas to the east of Cyprus a left-lateral motion with an eastward increasing of the tensional component (near the DSF) is predominant. Plate motion slip rates have been accurately determined by recent GPS data (McClusky et al., 2000 & 2003); a slip rate of ~6 mm/yr is associated to the northeastward motion of the African plate, whereas the northward motion of the Arabian plate has rate of ~18 mm/yr. The differential motion of Africa and Arabia relative to Eurasia is accommodated by the sinistral transpressional Dead Sea Transform Fault (DSF). The northward motion of the Arabian plate relative to Eurasia causes crustal shortening and thickening in Eastern Turkey.

### 3. Gravity data analysis

#### 3.1 Bouguer Gravity Data:

The Bouguer gravity anomaly map of the Eastern Mediterranean region, at a constant contour interval of 5

mGal (Fig. 3), has been regridded and prepared from the published maps (Gass and Masson-Smith, 1963; Woodside, 1976 & 1977; Egyptian General Petroleum Corporation (EGPC), 1980; Ginzburg et al., 1993; Makris and Wang, 1994; and Rybakov et al., 1997).

No detailed comment was made of the relative accuracies of the data presented, but it is noted that the agreement among data from various sources, in overlapping areas, is acceptable within the estimated error of  $\pm 5$  mGal. The compiled gravity data have been interpreted in terms of crustal structure on the basis of the available tectonic models in the region (e.g. Folkman, 1977; Woodside, 1976 & 1977; Ginzburg and Makris, 1979; and Segev et al., 2006).

A complete file of the datasets is available now on a web site at: <http://bgi.omp.obs-mip.fr/index.php/eng/Activities/Projects/World-Gravity-Map-WGM>. The WGM project is a gravity mapping project undertaken under the aegis of the Commission for the Geological Map of the World (CGMW) to complement a set of global geological and geophysical digital maps published and updated by CGMW, such as the World Digital Magnetic Anomaly Map (WDMAM), released in 2007. This new global digital map aims to provide a high-resolution picture of the gravity anomalies of the world, based on the available information on the Earth's gravity field.

The WGM project is conducted by the Bureau Gravimetric International (BGI), a center of the International Gravity Field Services (IGFS) of the International Association of Geodesy (IAG) with the support of the United Nations Educational, Scientific and Cultural Organization (UNESCO).

The gravity data compilation includes the available measurements issued from land, marine and airborne surveys and archived in the global database, as well as the new available gravity datasets collected from recent surveys or available in other global or regional databases. Major contributions to WGM include the official EGM08 global model, recently released by the National Geospatial-Intelligence Agency (NGA, USA), as well as the new global ocean gravity field derived from satellite altimetry (DNSC08 computed at the Danish National Space Centre and Sandwell and Smith models computed at Scripps Institution of Oceanography).

#### 3.2 Bouguer anomalies interpretation:

The Bouguer gravity anomaly map (Fig. 3) is presented for the region of the Eastern Mediterranean extending from the Northeastern Egyptian off-shore area in the south to southern Cyprus in the north. Bouguer anomalies in the Eastern Mediterranean (Fig. 3) are predominately positive, as might be expected for an oceanic area, however, they are substantially less positive than the Bouguer anomalies occurred in the Western Mediterranean or in deep ocean areas in general (Woodside and Bowin, 1970).

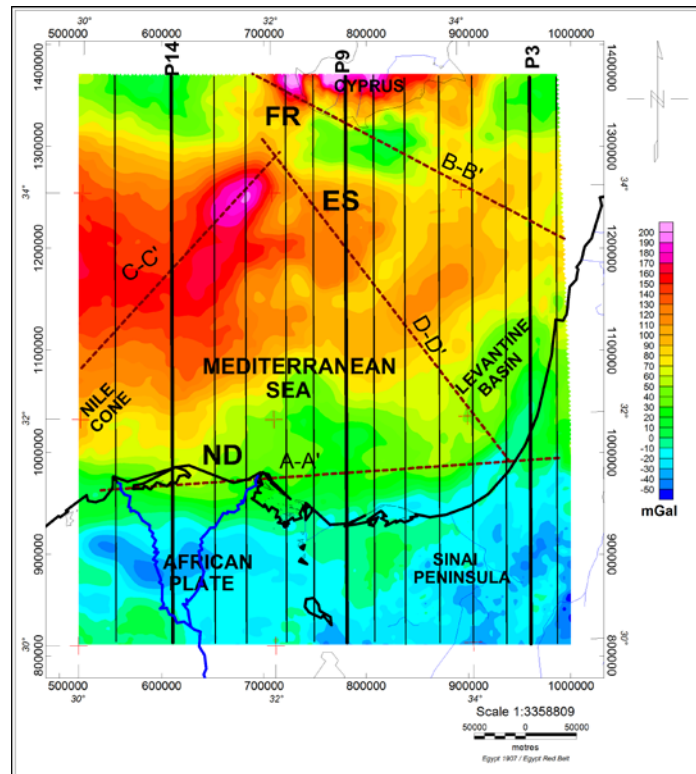


Figure (3): Bouguer grid data derived from the official Earth Gravitational Model (EGM2008) released by the National Geospatial Intelligence Agency (NGA). 3D gravity modeling profiles are also shown. AA', BB', CC', and DD' are location of modeling profiles shown in figure (9).

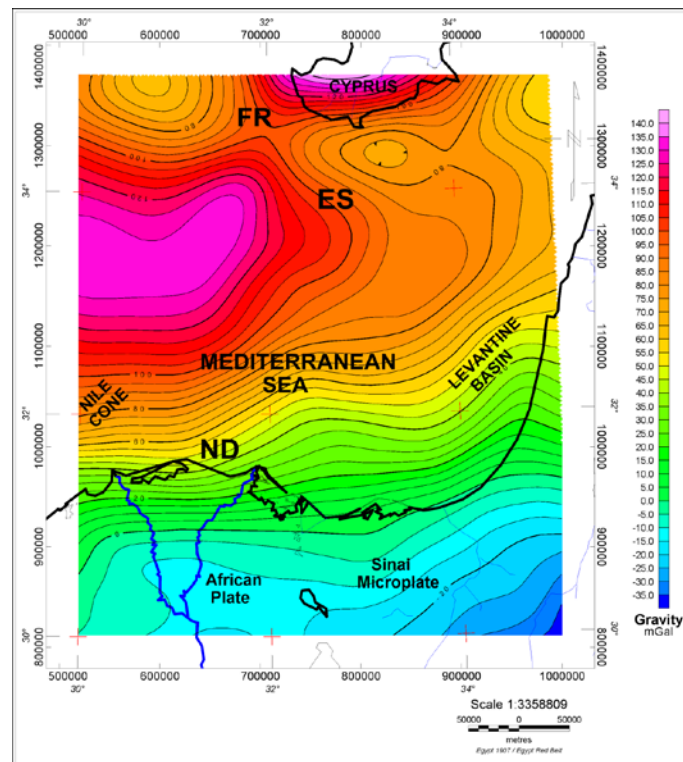


Figure (4): Regional Bouguer anomaly map of Eastern Mediterranean Sea using second order polynomial surface.

The map (Fig. 3) shows that there exists a considerable difference between the features of the gravity field over the Central and Southern Levantine Basin, Eratosthenes Seamount and South Florence Rise zone structure in the eastern, central and northwestern regions, respectively, and the Nile Delta and North Sinai in the south. The Levantine basin is characterized by a NNE-SSW trending high positive anomaly reaching Bouguer values of +135 mGal recorded between the eastern offshore of the Mediterranean and Eratosthenes Seamount, indicating a higher mass that was probably caused by uplifting of the Moho boundary by dynamic tectonic forces. Further west, the positive value is observed with +160 mGal below the South Florence Rise, which probably refers to a progressive crustal thinning towards the oceanic area

In the southern part, negative gravity values range from -30 mGal to +50 mGal beneath the Nile Delta (Nile Cone) and the South Levantine Basin is noticed, which may attribute to the thick sedimentary cover existing below these areas.. However, the negative anomaly value below northern Sinai of the study area explains clearly the increase of continental crustal thickness.

### 3.3. Separation of Bouguer data:

For geological interpretation, both the local and regional effects are separated. Therefore, the Bouguer gravity field of the studied area was subjected to isolation technique using the polynomial trend surface method. In the following, a brief account of the theoretical concepts of the polynomial trend surface method is presented:

The polynomial trend surface method is widely used by geologists, particularly in petroleum exploration, as a mean of separating a mapped variable into two components, the regional and residual trends. The trend corresponds to the concept of regional features, while residuals represent local features. This method is based on the assumption that, the spatial distribution of a particular phenomenon can be represented by some form of continuous surface, usually a defined geometric function. It is assumed that, an observed spatial pattern can be regarded as the summation of such a surface and a regional or residual term. The surface is a function of the two orthogonal coordinate axes; mathematically, this can be represented by (see Davis, 1973):

$$Z = f(x, y) + \epsilon \quad (1)$$

in which the variant  $Z$  at the point  $(x,y)$  is a function of the coordinate axes, plus the error term  $\epsilon$ . This expression is the generalized form of the general linear model, which is the basis of the most common trend methods. The function  $f(x,y)$  is expanded (approximated) with various terms to generate polynomial equations.

As a common example, consider fitting a trend surface as a polynomial regression, using  $(x,y)$  coordinates as the predictor variable. In the case of a cubic, the fit takes the form:

$$Z(x,y) = m_1 + m_2X + m_3Y + m_4XY + m_5X^2 + m_6Y^2 + m_7X^3 + m_8X^2Y + m_9XY^2 + m_{10}Y^3 \quad (2)$$

In this study, the regional trend was applied as either a first, a second or third order polynomial surface, in order to assess which order number was most specified and significantly the order number of the polynomial surface. A polynomial surface processing to the third order provides the best approximation to the observable gravity field. Thus, the trend of the regional field is separated from the observed gravity field.

### 3.4. Interpretation of the regional and residual gravity anomalies:

In Figures (4 and 5), respectively, the regional and residual Bouguer anomaly maps are displayed and plotted to show the deep and shallow structures in more detail. Generally, the regional field in the area under study is characterized by an oval shape and reveals that the orientation is mainly to ENE-WSW direction (Figure 4). It is considered to be mainly influenced by the density contrast between the crust and the upper mantle, and the undulating Moho discontinuity.

The regional anomaly field values generally decrease towards the E-W direction. This behavior trends reflect the effect of the transition from oceanic crust to continental crust of the Eastern Mediterranean towards the Arabian plate. In the northern part of Egypt, the regional anomaly shows an increase from -30 to +40 mGal. This indicates that, the crustal thickness decreases towards the Mediterranean Sea.

Figure (5) shows the residual gravity anomaly map with the alternatively high and low gravity anomalies of different orientations, gradients and shapes. This reflects the effect of the difference in density between the crystalline or igneous crust and the sediments, the variation of the basement geometry, and the effect of the bathymetric and topographic features. In the Levantine Basin, the negative residual gravity anomalies with a minimum value of -25 mGal are associated with the thick sedimentary sequences below the basin, as well as the negative anomalies of -35 mGal around Southern Cyprus. This is related to the structures of the sedimentary sequences and the basement geometry.

The residual gravity anomalies in the Eastern Mediterranean Basin are dominated by an elongated ENE-WSW trend with a maximum value of about +20 mGal, due to the density contrast between the oceanic crust and upper mantle beneath this region. There is a remarkable minimum in the residual gravity anomaly in the Gulf of Suez. This is due to the effect of the sedimentary cover, which has a thickness of 6 km (Said, 1962).

In the Nile Delta area, the negative residual gravity anomaly is -30 mGal, due to thick sediment sequences, especially beneath the northern part of the Nile Delta. A number of local residual gravity anomaly lows and highs are also apparent in the northwestern part of Arabia.

## 4. Three-dimensional modeling of the Bouguer anomalies

### 4.1. Methodological aspects:

The essential needed principles for the high resolution 3-D gravity modeling of the subsurface using the IGMAS program package, has been published by Götze and Lahmeyer (1988), that developed by Schmidt and Götze (1998). The area to be modeled is subdivided by a number of vertical planes. These planes vertices are defined and linked to lines separating two density complexes ( $\rho_1$  &  $\rho_2$ ). A line in one of the vertical planes separating density  $\rho_1$  &  $\rho_2$  is connected by a triangulation, with another line in the adjacent plane separating the same two densities. This forms a 3-D model of the subsurface structure.

Thus, the construction of the modeled bodies as polyhedrons bounded by plane surfaces and each of homogenous density leads to a good approximation of the geological structures. With the help of the Green and Gauss transformations, it is possible to calculate the exact attraction of 3-D bodies by transforming the volume integral into a surface and a line integral. When comparing the 2-D and 3-D models, the following factors, which are sometimes disregarded, should be born in mind with regard to the fitting and resolution of the models:

In the 2-D models, the longitudinal extent of a modeled structure should be three or five times its width (Jung, 1961). This implies that, all the cross sections of the underground model bodies are equivalent. This means that, the measured values reflect structures which theoretically have infinite extent perpendicular to the respective cross-section. In most cases, this is not true and the geophysical (gravity) values are made up of the superimposed gravity effects of numerous finite geological units ("sum effect of gravity"). Thus, the image of the subsurface structure produced by the 3-D model is more realistic.

The 3-D forward gravity-modeling package IGMAS (Interactive Gravity and Magnetic Analyzing System), that developed by Schmidt and Götze (1998), was used to establish the geometry and density distribution of the studied region. The 3-D geophysical modeling technique was applied for the Eastern Mediterranean region, covering an area of  $25 \times 10^4$  km<sup>2</sup> (500 km  $\times$  500 km).

### 4.2. Preparing the 3-D density model using gravity data:

The prior information required for the 3-dimensional gravity modeling includes the density or velocity distribution in the crust and upper mantle, the strike length, and the lateral, as well as the vertical extent of the causative bodies. The more the prior information, the less ambiguous will be the final gravity model. The initial model for the gross crustal structure of the Eastern Mediterranean is built out of 9 bodies (polygons) representing different lithologic and tectonic units. The location and orientation of the vertical

modeling planes are shown in Figs. (3 and 8). The direction of the vertical planes is perpendicular to the general geologic strike of the region. The vertical planes are parallel to each other, and the distances between the planes are changeable along the area of study, depending on the locations of the anomalies gradients, on the Bouguer map, their corresponding causative bodies, and on the geologic map. The data distribution has also been taken into consideration during the selection and orientation of the modeling planes along the investigated area.

The geometry of the initial model has been adopted from the results of the 2-dimensional gravity modeling and the previous seismic refraction-reflection sounding surveys conducted in the investigated area (Makris et al., 1983; Vidal et al., 2000; Ben-Avraham et al., 2002 & 2006; Ergün, 2005; Netzeband et al., 2006; and Longacre et al., 2007). Furthermore, an additional surface geologic and lithofacies information obtained from Said (1962) and El-Shazly (1974) were used. Deep boreholes data from Abdel Aal et al. (2001) were also considered for the Nile Delta region. Formation density compensated logs (FDC) of the deep oil and gas wells were also utilized for determining the bulk densities of the geological units composing the rock units of the sedimentary sections of the studied region.

### 4.3. Interpretation of three profiles across the study area:

Table (1) shows the different rock units used in the 3-dimensional gravity modeling and their respective densities. The description, as a result of the exploration wells in these areas (Mart and Robertson, 1998) and the geological units considered in the gravity model are identified with numbers. The density values used for the 3-dimensional gravity modeling of the studying area were estimated from the seismic velocities using the density-velocity relations (Figs 6 and 7), e.g. Christensen and Mooney, 1995 for the continental crust, Ludwig *et al.*, 1970; Hamilton, 1978; Carlson and Herrick, 1990; Hughes *et al.*, 1998 for the marine sediments. The new models demonstrate a lateral change from a normal continental crust across a zone of thinning and disappearance of the upper crust, to a relatively thin high velocity crust overlain by 14 km of sediments, with the Moho discontinuity located at a depth of 20-22 km (beneath the Levantine basin) of the gravity profiles.

Three sections from the eastern, middle and western sectors of the area of study is shown in Figures (8a, 8b and 8c) (refer to Figure 3 for the locations of the modeling planes). The gravity model incorporates the recent sediments of the basin floor. The negative residual anomaly is attributed to the sediments of the South Levantine Basin. The negative residual anomaly is well explained with a density value of 2000-2200 kg/m<sup>3</sup> for the shallowest (Pliocene-Quaternary) sediment rock unit. This density is also appropriate for the Upper Miocene evaporites dominated by halite. These two layers have been combined in the modeling.

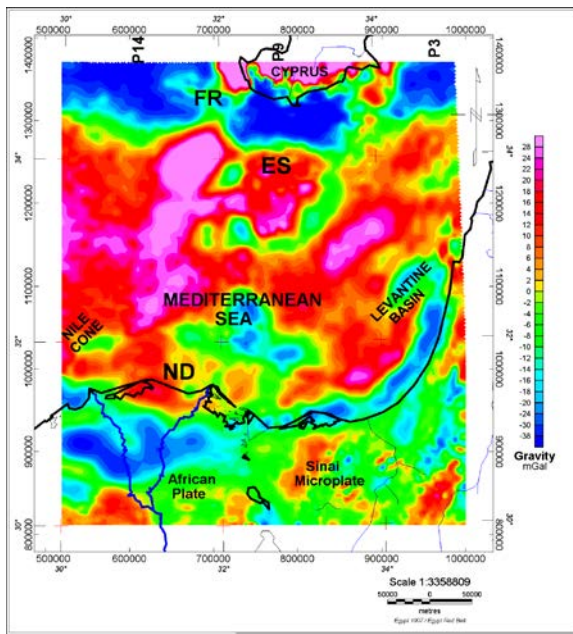


Figure (5): Residual anomaly map of Eastern Mediterranean Sea as derived using second order polynomial surface.

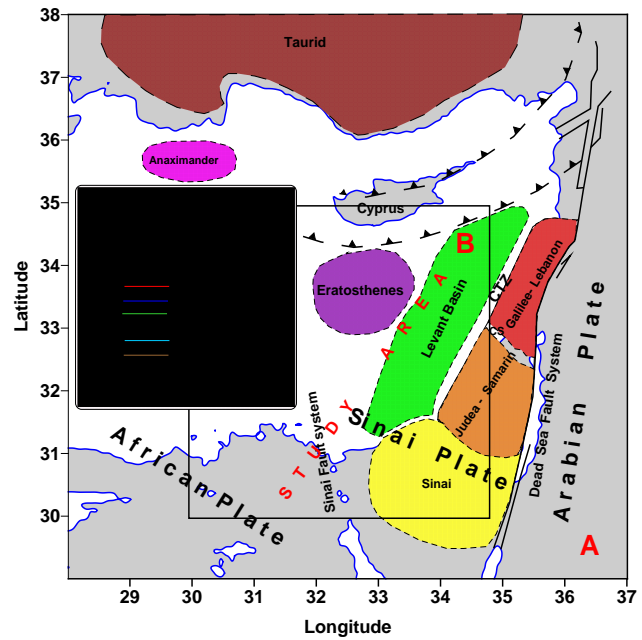


Figure (6): Tectonic scheme of the eastern Mediterranean (A) with generalized seismic sections (B). (A) after (Ben-Avraham et al. (2006)) and (B) Modified after (Ben-Avraham et al., 2002) and (Cohen et al., (1990)). CS, Carmel structure; CTZ, crustal transition zone.

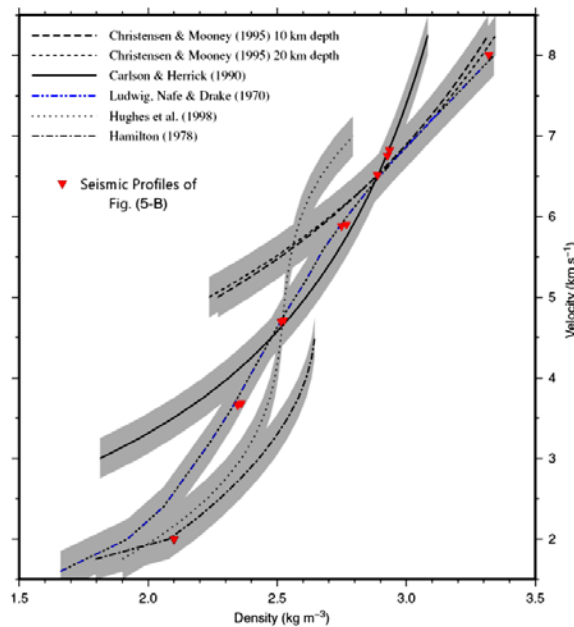


Figure (7): Relationship between velocity and density from Christensen & Mooney (1995) for continental crust, Ludwig et al. (1970), Hamilton (1978), Carlson & Herrick (1990) and Hughes et al. (1998) for marine sediments. Crosses indicate velocity and corresponding densities used for gravity modeling. Grey shaded areas mark the error bounds of  $0.25 \text{ g cm}^{-3}$ .



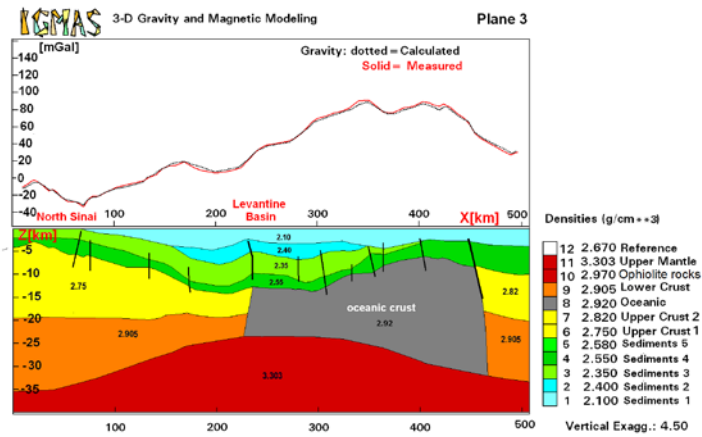


Figure (8a): The vertical cross section of the 3D gravity model from the eastern sector of the Eastern Mediterranean, along profile (P3). The lithological and/or structural boundaries are represented by bold black lines.

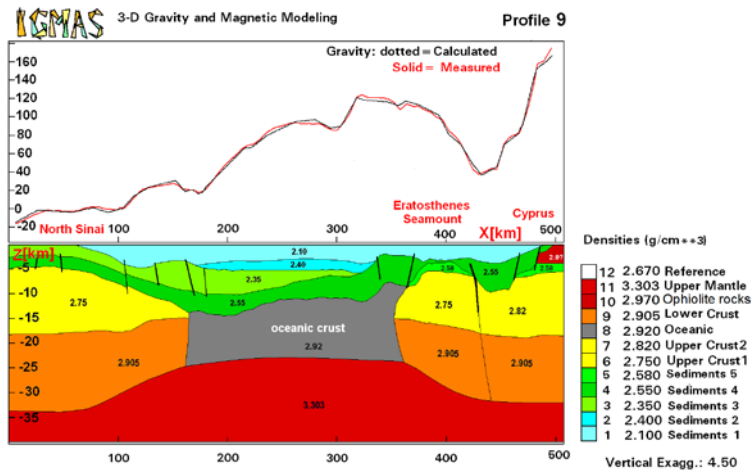


Figure (8b): The vertical cross section of the 3D gravity model from the middle sector of the Eastern Mediterranean, along profile (P9). The lithological and/or structural boundaries are represented by bold black lines.

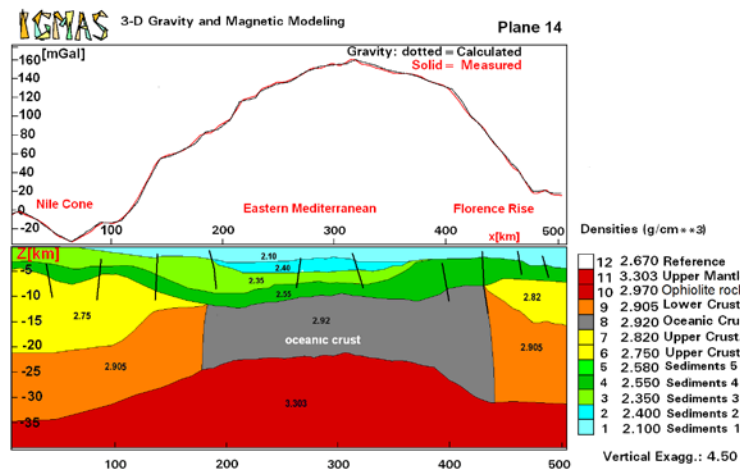


Figure (8c): The vertical cross section of the 3D gravity model from the western sector of the Eastern Mediterranean, along profile (P14). The lithological and/or structural boundaries are represented by bold black lines.

**Table (1): The P-wave velocities of the different rock units used in the 3-dimensional gravity modeling and their respective densities from the Eastern Mediterranean region (Makris et al., 1983; Vidal et al., 2000; Ben-Avraham et al., 2002 and 2006; Ergün, 2005; Netzeband et al., 2006; Longacre et al., 2007).**

No.	Geological Units	Description	Velocity Vp (km/s).	Density kg/m <sup>3</sup>
1	Sedimentary 1	Pliocene-Quaternary sediments.	1.9–2.1	2100
2	Sedimentary 2	Evaporitic sediments..	4.3–4.4	2400
3	Sedimentary 3	Pre-Evaporitic sediments..	3.60	2350
4	Sedimentary4	Clastic compact sediment	4.4	2550
5	Sedimentary5	Messinian compact sediment.	4.8	2580
6	Upper crust1	Granitic rocks	6.0–6.3	2750
7	Upper crust2	Granitic rocks	6.4	2820
8	Oceanic crust	Basaltic rocks	6.8	2920
9	Lower crust	V. compacted granitic rocks	6.7	2905
10	Troodos Ophiolite	Ophiolite rocks	6.90	2970
11	Normal Upper mantle	Peridotite rocks,	8.00	3303

Deeper sediments include indurated Miocene and older sediments, for which we have limited velocity information; we have assumed densities of 2400, 2350, 2550 and 2580 kg/m<sup>3</sup> for these units. Despite the uncertainties in these assumptions, the bulk densities used agree with those observed locally in (relatively shallow) the samples from ODP drill holes on the Florence Rise (Erickson, 1978) and well correlated with the refraction-reflection results (Ginzburg and Ben Avraham, 1987; and Netzeband, 2006). The total thickness of the sediments in the studied area, as obtained from the gravity modeling, is relatively 14 km (Fig. 8). The rocks, sparsely deposited, increase the thickness towards the central part of the Mediterranean region, especially toward the southern part of the Levantine Basin

For the basement rock units, we distinguish between those places, where we assume oceanic crust is present and those where a continental crust is more likely. Makris et al. (1983), Marzouk, (1988) and Netzeband et al. (2006) established the upper crustal basement velocities of 6.0-6.4 km s<sup>-1</sup> in the thick crust of North Sinai, Nile Delta, Eratosthenes Seamount and South Cyprus, with deeper units of 6.7 km s<sup>-1</sup> (lower crust) and 8.0 km s<sup>-1</sup> for the mantle. The crust and upper mantle were modeled, using the corresponding densities of 2750-2820, 2900 and 3330 kg/m<sup>3</sup> for these three units. Since the velocity of 6.0 km s<sup>-1</sup> corresponds to a typical continental upper crust of a broadly granitic nature (Kearey and Vine, 1996).

The Cyprus high correlates approximately with the location of the Troodos ophiolite (Gass and Masson-Smith, 1963), and the extension of the high to the east and west indicates likely continuation of the ophiolite at a depth below the younger sediments of the Latakia and southern Antalya Basins. Velocities of the crustal basement units are available from the local work of Makris et al. (1983), De Voogd et al. (1992), and from

the general models of continental and oceanic crusts (see summary in Kearey and Vine, 1996). We also used this density for the known ophiolites, such as Troodos, and their likely offshore extensions.

The upper continental crustal unit generally thickens southward to the African Plate. Its maximum thickness has been observed beneath both Sinai and northern Egypt in 6 km depth and becomes 25 km depth. The gravity crustal structure models show that, the continental-oceanic crustal boundary is rather gradual in the south and occurs beyond the continental margin, at the base of the continental slope. On the other hand, to the north, the continental-oceanic crustal structures are much sharper and occur near the shore.

The existing of an oceanic crust (with a density value of 2920 kg/m<sup>3</sup>) in the Levantine Basin is rather significant, because of the small size of the basin. This crust is probably quite old, at least Triassic or Early Jurassic, that is the age suggested for the rifting of the South Levant margin. Along the Levant margin, the transition zone between oceanic and continental crusts forms a zone of weakness which, can be activated due to the stress transmission from the collision zone in the north (Ben-Avraham, 1978).

The model shows that, the top of this oceanic crust in the central part of the profiles is relatively flat at a mean depth of 13 km. The model exhibits also the presence of a steep increase in the crustal thickness toward the continent below the coastal plain.

The Moho depth map (Figure 8c) reveals a relatively medium depth of 28 km beneath the South Florence rise in the northwest, which lies at a constant depth of 20 to 23 km below the Levantine Basin at the central part of the study area, indicating thinning of the earth's crust in the northern part of the area. The model reveals also a maximum Moho depth of about 33-35 km beneath both Northern Egypt and Northern Sinai, respectively.

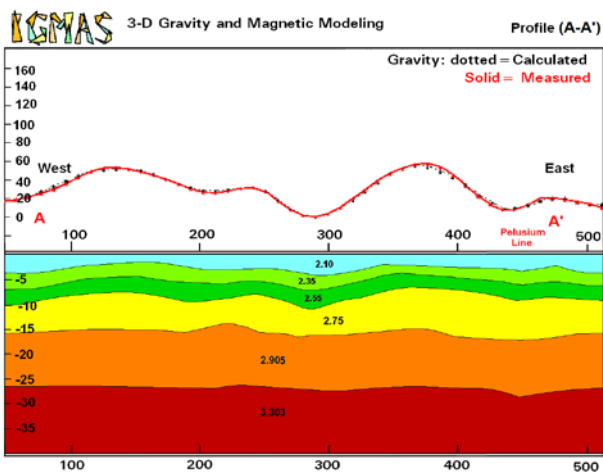


Figure (9 a): The vertical cross section of the 3D gravity model (AA'). The location of modeling profile is shown in figure (3). It was projected running from west to east parallel to the coastal area. It is cutting the northern Nile Delta and southern border of Levantine basin.

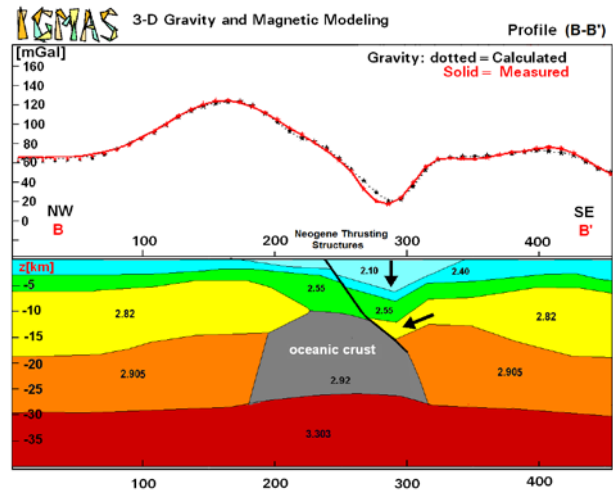


Figure (9 b): The vertical cross section of the 3D gravity model (BB'). The location of modeling profile is shown in figure (3). It was possibly expected that the sedimentary thickness increase towards the Cypriot Arc thrust zone, whereas, decreasing the crustal thickness indicating a collision taking place between African and Eurasian plates; the results were also consistent with the regional crustal values.

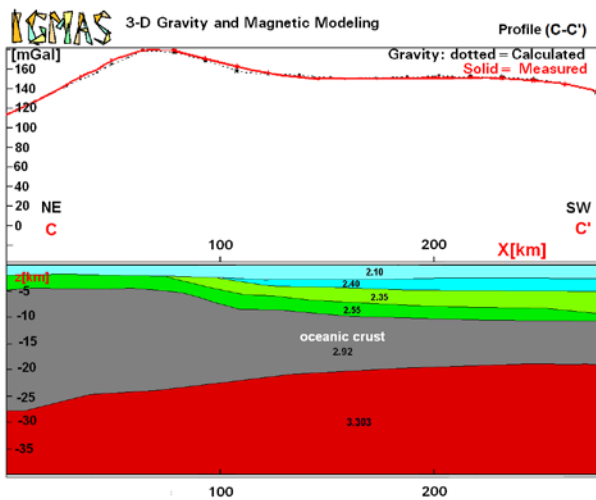


Figure (9 c): The vertical cross section of the 3D gravity model (CC'). This model located in the north west of the study area and trended NE-SW. The crust is fully oceanic and its thickness increase, toward the Florence Rise anomaly, as shown in Fig. 3.

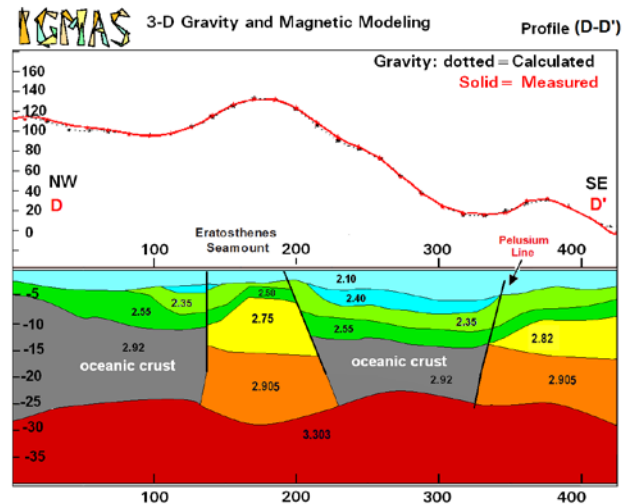


Figure (9 d): The vertical cross section of the 3D gravity model (DD'). The location of Pelusium tectonic shear zone separates the continental crustal layer from the oceanic one along the Israeli coastal region. Moreover, the model shows that, the Eratosthenes Seamount (elastic high) was modeled as a separate continental block bounded by two oceanic boundaries from SE and NW. This block is in the process of actively subsiding, breaking-up and being thrust, beneath both Cyprus to the north and the Levantine Basin to the south

Densities (g/cm<sup>3</sup>)

12	2.670	Reference
11	3.303	Upper Mantle
10	2.970	Ophiolite rocks
9	2.905	Lower Crust
8	2.920	Oceanic Crust
7	2.820	Upper Crust2
6	2.750	Upper Crust1
5	2.580	Sediments 5
4	2.550	Sediments 4
3	2.350	Sediments 3
2	2.400	Sediments 2
1	2.100	Sediments 1

Vertical Exagg.: 4.50

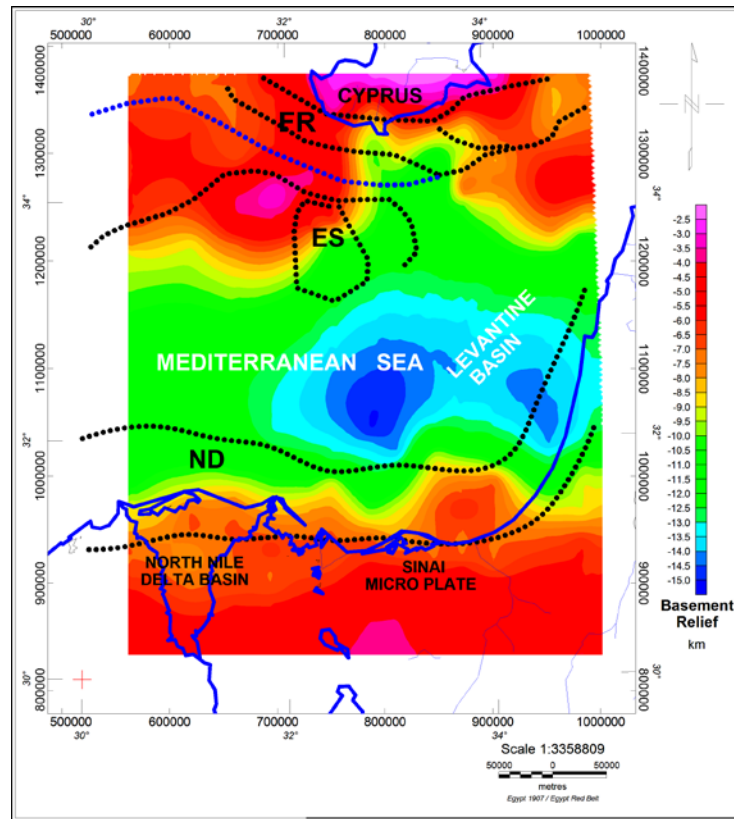


Figure (10 a): Basement Relief (sedimentary thickness) map obtained in this study. Abbreviations are: FS- Florence Rise, ES- Eratosthenes Seamount and ND- Nile Delta. Note that the basement relief was found to decrease towards Cyprus to the north.

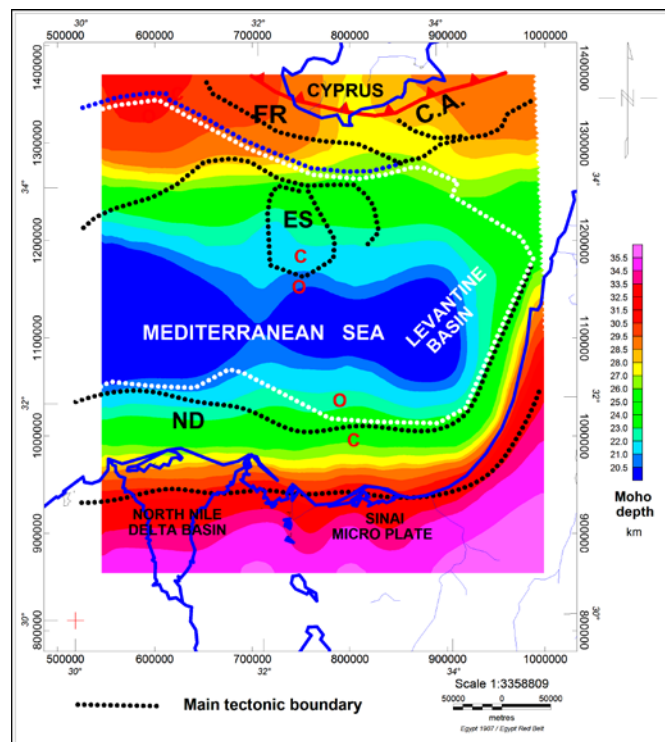


Figure (10 b): Moho depth Map of the study area. FS- Florence Rise, ES- Eratosthenes Seamount and ND- Nile Delta White bold dots line is approximate boundary between oceanic (O) and continental (C) crust derived from this study. It is noted that the crustal thickness was found to increase towards the Cypriot Arc thrust zone in agreement with gravity interpretation; the results were also consistent with the regional crustal values.

## 5. DISCUSSIONS

This study is an attempt to achieve a better understanding of the tectonic setting in the complex region of the Eastern Mediterranean. Crustal structure, thickness of rock units, the transition between the oceanic and continental crusts and the regional integrated model of the gravity field in the area are investigated. The study is based on detailed 3-D gravity modeling (as shown in Fig. 9, AA', BB', CC' and DD' cross sections), where the estimated densities are projected using IGMAS software. Depths in Figure (9) are comparable to the two maps (basement relief and Moho depth maps) in Figures (10a and 10b).

Generally, the Nile Delta and North Sinai areas are marked by east-west trending linear anomaly with gravity low. They are characterized by very thick continental crustal thickness with a thin sedimentary cover (Figure 10a). Along the entire study region, the Nile Delta and North Sinai areas represent the deepest region of the Moho discontinuity (with Moho depth of ~30-35 km, as shown in Figure 10b). Whereas the Northeastern Egyptian coastal area, as illustrated in the 3-D gravity profiles and Moho depth map (shown in Figs 8, 9a and 10b), is characterized by very steep transitional crustal layer (16-19 km thick) with a thick sedimentary cover (nearly of ~8-11 km), which is relatively thicker than the previous zone. The Moho beneath this area is modeled of intermediate-depth ~26-28 km. The upper continental crust got very thin through this transition zone (~6 km thick).

In the Eastern Mediterranean and the Levantine Basin, which is extending from 32° to 34° N, is mostly characterized by oceanic crust (as shown in Fig. 8 and 10b). The sedimentary cover is very thick beneath the Levantine basin (~14 km thick).

In general, the 3D density profiles interpretations explain the crustal type variation (continental and/or oceanic) along the region of the northeastern Egyptian coastal zone, including North Sinai and the Nile Delta in the southern part, extending northward to the Levantine basin, the Eratosthenes seamount and south Cyprus.

The obtained continental crust got thicker (with Moho depth of 30-34 km) beneath Sinai, Nile Delta and south Cyprus (Figs. 8 and 12b). The sedimentary cover was modeled for both Levantine Basin and Eratosthenes Seamount with almost ~14 km and ~6 km beneath the two areas respectively (Fig. 12a).

Gravity data show a higher Bouguer anomaly in Cyprus with respect to the Eratosthenes seamount (Khair & Tsokas, 1999). These anomalies may be caused by combination of various tectonic sources that are located at different depths (e.g., may be caused by varying combinations of ophiolites and thinning sediments as estimated from the 3-D gravity modeling).

The issue about the continental or oceanic nature of the crust beneath the Eratosthenes seamount and the Levantine basin is still a matter of discussion. From results in Figure (8, 9 and 10) we conclude that the crust

beneath the Eratosthenes Seamount is almost continental crust, as many authors suggest (BenAvraham *et al.*, 2002, Di Luccio *et al.*, 2007 and many reference therein) and whose thickness varies in the range 22-26 km.

The existence of continental type crustal blocks in the eastern Mediterranean basin is due, as suggested by many authors, to the rifting from the African continental crust (BenAvraham *et al.*, 2002 and reference therein).

## 6. CONCLUSIONS

The compiled Bouguer anomaly map of Eastern Mediterranean enabled us to establish a possible density model along the South Eastern Mediterranean region including the African boundary of Egyptian coast of Nile Delta and Sinai, South Levantine Basin, Eratosthenes Seamount, Florence Rise and southern region of Cyprus. The gravity data have proved to be useful for delineating shallow and deep structures and helping the definition of models which agree with the basic information supplied by the previous geophysical investigations, as well as, from geological knowledge. The Bouguer anomaly map of the study area is characterized by the presence of different anomalies that differ in their amplitudes, sizes and trends. These anomalies are caused by combination of various tectonic sources that are located at different depths. The main important contributions of this work are defining and estimate the nature and state of the crustal structure of the study area.

In general, the features of the gravity field such as the gradients and elongated anomalies can be divided into three groups according to their trends: The first group oriented in ENE-WSW and influenced by the density contrast between the crust and upper mantle. The second group, oriented in NE-SW direction parallel to the coastal line, reflects mainly the thickness variations of the Tertiary sediments. The third group, oriented NW-SE may be related to the young tectonic dislocations.

On the Egyptian coast, the changes in the crust, sediment and upper mantle are very intense as obtained from the 3-D gravity modeling. The crust is still continental, only 21 km thick and at least in some areas, covered by thin sediments. The density of the continental crust is 2750 kg/m<sup>3</sup>. A few kilometers farther to the north the thickness of crust decreases abruptly (transition zone). This region is occupying a very narrow zone parallel to the coastal region of the Mediterranean. Further to the north, the nature of the crust changes completely. We find an oceanic crust only 10 km thick (without the thick sediments) which seems to cover large parts of the South Levantine Basin. Close to the shear subduction zone, the gravity high of Cyprus is caused by varying combinations of ophiolites and thinning sediments as estimated from the 3-D gravity modeling.

The Eratosthenes Seamount (with continental crustal type) is in the process of actively subsiding, breaking-up and being thrust, beneath both Cyprus to the north and the Levantine Basin to the south. This incipient collisional process was confirmed by existing the Plio-Quaternary uplift of the Troodos ophiolite. Comparison with the geology of southern Cyprus and offshore areas suggests a link between northward underthrusting of the Eratosthenes Seamount and late Pliocene-mid Quaternary uplift of southern Cyprus, focused on the centre of the Troodos ophiolite (Robertson et al, 1995).

The estimated oceanic-continental crustal border is coincident with the African plate boundary in the Eastern Mediterranean region. Moreover, the Eratosthenes Seamount is characterized by a continental crustal type and was outlined as a separated continental block with Moho depth of 22-26 km.

It was observed an inverse correlation between sediment and crustal thickness, observed in extensional tectonic regimes (Ritzmann *et al.*, 2007), where thinned crust acquires correspondingly thicker sedimentary column. This inverse correlation cannot be considered valid for oceanic areas in this study (such as also those in Western Mediterranean, see e.g. the central Tyrrhenian Sea or Ionian Sea, (e.g. Gaulier et al., 1997 and Doglioni, 1999). Moreover, accretion zones in collisional tectonic environment wouldn't allow a straightforward extension of the statement. Good example of such situation at the place where the collision zone (thrusting) is modeled beneath south Cyprus as revealed in Fig. 9b. Expected complicated thick sedimentary sequences have been formed. The parental continental crust is in the gradual deepening and thinning in later stages near the thrusting contact. Thus formations of transitional and oceanic type crust beneath the thrusting zone were developed. At early stage, these systems might have looked like active continental-oceanic boundary, which then evolved in a complex collision system.

## 7. ACKNOWLEDGMENTS

We would like to express my gratitude to Dr. Sabine Schmidt for her help and permit using IGMAS software. We thank also, Prof. Michele Pipan, University of Trieste, Italy for his critical and constructive comments that greatly contributed to improving this work

## REFERENCES

- Abdel Aal, A., El Barkooky, A., Gerrits, M., Meyer, H., Schwander, M., Zaki, H., 2001.** Tectonic evolution of the Eastern Mediterranean Basin and its significance for hydrocarbon prospectively in the ultra deepwater of the Nile Delta. *Lead. Edge* 19, 1086–1102.
- Aksu, A. E., J. Hall and C. Yaltirak, 2005.** Miocene to recent tectonic evolution of the eastern Mediterranean: New pieces of the old Mediterranean puzzle, *Marine Geology*, 221, 113.
- Ben-Avraham, Z., (1989)** Multiple opening and closure of the Eastern Mediterranean and south China Basins. *Tectonics*, Vol. 8, No. 2, Pp. 351-362.
- Ben-Avraham, Z., A. Ginzburg, J. Makris and L. Eppelbaum, 2002.** Crustal Structure of the Levant Basin, Eastern Mediterranean," *Tectonophysics*, Vol. 346, No. 1-2, 2002, pp. 23-43. Doi:10.1016/S0040-1951(01) 00226-8.
- Ben-Avraham, Z., U. Schattner, M. Lazar, J. K. Hall, Y. Ben-Gai, D. Neev, and M. Reshef, 2006.** Segmentation of the Levant continental margin, eastern Mediterranean, *Tectonics*, 25, TC5002, doi:10.1029/2005TC001824. Biju-Duval, J. Letouzey et L. Montadert, 1976: Structure and evolution of the Mediterranean basins, IFP internal report, 56 p.
- Ben-Avraham, Z.; Nur, A. and Cello, G., 1987.** Active transcurrent fault system along the north African passive margin. *Tectonophysics*, Vol. 141, Pp. 249-260.
- Biju-Duval, B.; Letouzey, J. and Montadert, L., 1978.** Structure and evolution of the Mediterranean basins. In: Hsue, K. and Montadert et al. (Editors), *Initial Report of the Deep Sea Drilling project*, Vol. 42, Part 1, Pp. 951-984.
- Carlson, R. L. & Herrick, C. N., 1990.** Densities and porosities in the oceanic crust and their variations with depth and age, *J. Geophys. Res.*, 95, 6, pp. 9153–9170.
- Christensen, N. and Mooney, W. 1995.** Seismic velocity structure and composition of the continental crust: A global view. *Journal of Geophysical Research* 100(B6): doi: 10.1029/95JB00259. issn: 0148-0227.
- Cordell, L. and Grauch, V.J.S., 1985.** Mapping basement magnetization zones from aeromagnetic data in the Saint Juan Basin, New Mexico. In (William J. Hinze, Ed.), *The Utility of Regional Gravity and Magnetic Anomaly Maps*. SEG, Tulsa, OK, pp. 181–197.
- Cohen, Z., V. Kaptan and A. Flexer, 1990.** The Tectonic Mosaic of the Southern Levant: Implications for Hydrocarbon Prospects, *Journal of Petroleum Geology*, Vol. 13, No. 4, pp. 437-462. Doi:10.1111/j.1747-5457.1990.tb00858.xsl;
- Davis, J., 1973. *Statistics and data analysis in geology*: John Wiley and Sons, New York.
- De Voogd, B., Truffert, C., Chamot-Rooke, N., Huchon, P., Lallemand, S., Le Pichon, X., (1992)** Two-ship deep seismic sounding in the basins of the Eastern Mediterranean Sea (Pasiphae Cruise). *Geophys. J. Int.* 109, 536– 552.

- Dercourt, J., L. P., Zonenshain, L. E., Ricou, V.G. Kazmin, X. Le Pichon, A.L. Knipper, C. Grandjacquet, I.M. Sbertshikov, J. Geysant, C. Lepvrier, D.H. Pechersky, J. Boulin, J.-C. Sibuet, L.A. Savostin, O. Sorokhtin, M. Westphal, M.L. Bazhenov, J.P. Lauer and B. Biju-Duval (1986)** Geological evolution of the Tethys belt from the Atlantic to the Pamirs since the Lias, *Tectonophysics*, vol. 123, pp. 241-315.
- Dewey, J.F., Pittman, III, W.C., Ryan, W.B.F., Bonnin, J., 1973.** Plate tectonics and the evolution of the Alpine system, *Geological Society of America Bulletin*, vol. 84, , pp. 3137-3180.
- Di Luccio, F. and Pasyanos, M. E., 2007.** Crustal and upper-mantle structure in the Eastern Mediterranean from the analysis of surface wave dispersion curves, *Geophysical Journal International*, Volume 169, Issue 3, pages 1139–1152, June 2007
- Dogliani, C., Gueguen, E.P. Harabaglia, P., Mongelli, F., 1999.** On the origin of west-directed subduction zones and applications to the western Mediterranean, *Geological Society, London, Special Publications* January 1, 1999, v. 156, p. 541-561, doi: **10.1144/GSL.SP.1999.156.01.24**
- Dolson J., Shann, M., Matbouly, S., Harwood, C., Rashed, R., and Hammonds, H., 2004 a.** The petroleum potential of Egypt, in Downey M., Threet, J., and Morgan, W., eds., *Petroleum Provinces of the Twentyfirst Century*, American Association of Petroleum Geologists Memoir 74, pp. 453-482.
- Dolson, J.C., Boucher, P.J., Dodd, T., and Ismail, J., 2004b.** Petroleum potential of an emerging giant gas province, Nile Delta and Mediterranean Sea off Egypt, *Oil & Gas Journal*, vol. 100, no. 20, pp. 32-37.
- Egyptian General Petroleum Company (EPC), 1984.** Bouguer Anomaly map of Nile Delta and north Sinai, (scale: 1: 100,000)
- El Shazly, E.M., Abdel Hady, M.A., El Kassas, I.A., El Shazly, M.M., 1974.** Geology of Sinai Peninsula from ERTS-2 satellite images. *Rem. Sens. Center, Cairo*. 10 pp.
- Endrun, B., Meier, T., Bischoff, M. and Harjes, H.P. 2004.** Lithospheric structure in the area of Crete constrained by receiver functions and dispersion analysis of Rayleigh phase velocities, *Geophys. J. Int.*, 158, 592608.
- Ergün, M., S Okay, C Sari, E Zafer Oral, M Ash, 2005.** Gravity anomalies of the Cyprus Arc and their tectonic implications, *Marine Geology*, Volume 221, Issues 1–4, Pages 349–358
- Folkman Y., 1977.** Magnetic and gravity investigation of the crustal structure of Israel, Ph. D. thesis, Tel Aviv University (in Hebrew).
- Garfunkel, Z., 1998.** Constrains on the origin and history of the Eastern Mediterranean basin, *Tectonophysics*, vol. 298, pp. 5-35.
- Garfunkel, Z., 2004.** Origin of the Eastern Mediterranean basin: a reevaluation. *Tectonophysics* 391, 11–34.
- Gass, I.G., and D. Masson-Smith, D., 1963.** The geology and gravity anomalies of the Troodos massif, Cyprus. *Philosophical Transactions of the Royal Society of London, Series A: Mathematical and Physical Sciences*, v. 255, n. 1060, p. 417-467.  
(<http://www.library.illinois.edu/orr/get.php?instid=182763>)
- Gaulier, J.M, Chamot-Rooke, N. and Jestin, F., 1997.** constraints on Moho Depth and Crustal Thickness in the Liguro-Provençal Basin from a 3D Gravity Inversion : Geodynamic Implications, *Oil & Gas Science and Technology - Rev. IFP*, Vol. 52 (1997), No. 6, pp. 557-583, DOI: 10.2516/ogst:1997060
- Ginzburg A. & Makris J, 1979.** Gravity and density distribution in the Dead Sea rift and adjoining areas. *Tectonophysics*, 54, T17-25,
- Gizburg A., Folkman Y. , Rybakov M., Rotstein Y., Assael R., and Yuval Z., 1993.** Israel Gravity Map and Regional Bouguer Gravity Map, scale 1:500,000, prepared and printed by the survey of Israel.
- Götze, H.J. and Lahmeyer, B., 1988.** Application of 3-D interactive modeling in gravity and magnetics. *Geophysics*, 53, 1096-1108.
- Hamilton, E.L., 1978.** Sound velocity-density relations in the sea-floor sediments and rocks, *J. Ac. Soc. Am.*, 63, pp. 366–377.
- Harrison R., Newell W., Batuhanlı H., Panayides I., McGeehin, J., Mahan, S., Özhür, A., Tsiolakis, E. and Necdet, M., 2004.** Tectonic framework and late Cenozoic tectonic history of the northern part of Cyprus: implications for earthquake hazards and regional tectonics, *Journal of Asian Earth Sciences*, Vol. 23, pp. 191-210
- Harrison, F., 2008.** A Model for the Plate Tectonic Evolution of the Eastern Mediterranean Region that Emphasizes the Role of Transform (Strike-Slip) Structures, 1<sup>st</sup> WSEAS International Conference on ENVIRONMENTAL and GEOLOGICAL SCIENCE and ENGINEERING (EG'08) Malta, September 11-13, 2008
- Harrison, R. and Panayides, I., 2004.** A restraining-bend model for the tectonic setting and uplift of Cyprus, in Chatzipetros, A.A. and Pavlides, S.B. (eds.), *Proceedings of the 5<sup>th</sup> International Symposium on Eastern Mediterranean Geology*,

- Thessaloniki, Greece, 14 to 20 April, 2004, pp B43-B46.
- Hofstetter, A and Bock G., 2004.** Shear-wave velocity structure of the Sinai subplate from receiver function analysis, *Geophysical Journal International*, Volume 158, Issue 1, pages 67–84, DOI: 10.1111/j.1365-246X.2004.02218.x
- Hughes, S., Barton, P.J., & Harrison, D., 1998.** Exploration in the Shetland-Faeroe Basin using densely spaced arrays of ocean-bottom seismometer, *Geophys.*, 63, 2, pp. 328–334.
- Jackson J., and McKenzie, D., 1988.** The relationship between plate motions and seismic moment tensors, and the rates of active deformation in the Mediterranean and Middle East, *Geophysical Journal*, vol. 93, pp. 45-73.
- Jung, K. (1961).** *Schwerkraftverfahren in der angewandten Geophysik.* Akademische Verlagsgesellschaft Geest & Portig, Leipzig, 348 Seiten.
- Karagianni, E.E., C.B. Papazachos, D.G. Panagiotopoulos, P. Suhadolc, A. Vuan and G.F. Panza, 2005.** Shear velocity structure in the Aegean area obtained by inversion of Rayleigh waves, *Geophys. J. Int.*, 160, 127143.
- Kastens, K., (1991).** Rate of outward growth of the Mediterranean ridge accretionary complex. *Tectonophysics*, 199, Pp. 25-50.
- Kearey, P., Vine, F., 1996.** *Global Tectonics.* Blackwell Publishing. 344 pp.
- Kempler D., 1994.** Tectonic patterns in the easternmost Mediterranean (Ph.D. thesis). Hebrew Univ.
- Kempler D., 1998.** Eratosthenes Seamount: the possible spearhead of incipient continental collision in the eastern Mediterranean Sea, in Robertson, A. H. F., et al., ed., *Proceeding of the oceanic drilling program, scientific results*, vol. 160, p709-721.
- Kempler, D., and Ben-Avraham, Z., 1987. The Tectonic evolution of the Cyprian Arc., *Annales Tectonicae*, Vol. 1, P 58-71.
- Kempler, D., and Garfunkel, Z., 1995.** Constraints on Afroarabia-Eurasia lithosphere consumption since 80 Ma. 2<sup>nd</sup> Int. Symp. On the geology of eastern Mediterranean Region, 11.
- Khair, K., and G.N. Tsokas, 1999.** Nature of the Levantine (eastern Mediterranean) crust from Multiplesource Werner deconvolution of Bouguer gravity anomalies, *J. Geophys. Res.*, 104(B11), 25,46925,478.
- Koulakov, I., and S.V. Sobolev, 2005.** Moho depth and three dimensional P and S structure of the crust and uppermost mantle in the Eastern Mediterranean and Middle East derived from tomographic inversion of local ISC data, *Geophys. J. Int.*, doi: 10.1111/j.1365246X.2005.02791.x.
- Lev Eppelbaum and Youri Katz, 2011.** Tectonic-Geophysical Mapping of Israel and the Eastern Mediterranean: Implications for Hydrocarbon Prospecting Open Access. PP.36-54 *Positioning*, 2011, 2, 36-54 doi:10.4236/pos.2011.21004 Published Online February 2011 (<http://www.SciRP.org/journal/pos>)
- Longacre, M., Bentham, P., Hanbal, I., Cotton, J., Edwards, R., 2007.** New Crustal Structure of the Eastern Mediterranean Basin: Detailed Integration and Modeling of Gravity, Magnetic, Seismic Refraction, and Seismic Reflection Data. *EGM Innovation in EM, Gravity and Magnetic Methods: a new Perspective for Exploration*, Capri, Italy, April 15–18.
- Ludwig, J. W., Nafe, J. E., & Drake, C. L., 1970.** Seismic refraction, *The Sea*, 4, 1, pp. 53–84.
- Ludwig, W.J., Nafe, J.E., and Drake, C.L., 1970,** Seismic refraction, in *The Sea*, A.E. Maxwell (Editor), Vol. 4, Wiley-Interscience, New York, pp. 53-84.
- Makris, J., and T. Yegorova, 2005.** A 3D density velocity model between the Cretan Sea and Libya, *Tectonophysics*, doi:10.1016/j.tecto.2005.11.03.
- Makris, J., Ben-Avraham, Z., Behle, A., Ginzburg, A., Giese, P., Steinmetz, Whitmarsh, R. B., and Eleftheriou, S., 1983.** Seismic reflection profiles between Cyprus and Israel and their interpretation. *Geophys. J. R. Astron. Soc.* 75, 575–591.
- Makris, J., Wang, J., 1994.** Bouguer gravity anomalies of the eastern Mediterranean Sea. In: Krashennikov, V.A., Hall, J.K. (Eds.), *Geological Structure of the Northeastern Mediterranean (Cruise 5 of the Research Vessel "Akademik Nikolaj Strakhov")*. Historical Production Hall Ltd., Jerusalem. Pp. 87–98
- Marone, F., M. van der Meijde, S. van der Lee and D. Giardini, 2003.** Joint inversion of local, regional and teleseismic data for crustal thickness in the EurasiaAfrica plate boundary, *Geophys. J. Int.*, 154, 499514.
- Marsouk, I.A., 1988.** Study of crustal structure of Egypt deduced from deep seismic and gravity data, Ph.D. dissertation thesis: University of Hamburg, 118pp.
- Mart, Y., and Robertson, A.H.F., 1998.** Eratosthenes Seamount: an oceanographic yardstick recording the late Mesozoic–Tertiary geological history of the Eastern Mediterranean. In Robertson, A.H.F., Emeis, K.-C., Richter, C., and Camerlenghi, A. (Eds.), *Proc. ODP, Sci. Results*, 160: College Station, TX (Ocean Drilling Program), 701–708. doi:10.2973/odp.proc.sr.160.034.1998.



- McClusky S., and 27 others., 2000.** Global positioning system constraints on plate kinematics and dynamics in the eastern Mediterranean and Caucasus, *Journal of Geophysical Research*, vol. 105, no. 5, pp. 5,695-5,719.
- McClusky, S., R. Reilinger, S. Mahmoud, D. Ben Sari, and A. Tealeb, 2003.** GPS constraints on Africa (Nubia) and Arabia plate motion, *Geophys. J. Int.*, 155, 126–138, doi:10.1046/j.1365-246X.2003.02023.x.
- McKenzie, D.P., 1970.** Plate tectonics in the Mediterranean region, *Nature*, 226, pp: 239-243
- Meier, T., K. Dietrich, B. Stöckhert and H. P. Harjer, 2004.** Onedimensional models of shear wave velocities for the eastern Mediterranean obtained from the inversion of Rayleigh wave phase velocities and tectonic implications, *Geophys. J. Int.*, 156, 4558, doi: 10.1111/j.1365246X.2004.02121.x.
- Neev, D., G. Almogor, A. Arad, A. Ginzburg, and J. K. Hall, 1976.** The geology of the southeastern Mediterranean Sea, *Bulletin*, 51 pp., vol. 68, G.S.I., Jerusalem.
- Netzeband, G.L., Gohl, K., Hübscher, C.P., Ben-Avraham, Z., Deghani, G.A., Gajewski, D., Liersch P., 2006.** The Levantine Basin-crustal structure and origin, *Tectonophysics*, 418, 167–188,
- Nur, A. and Ben-Avraham, Z., 1978.** The Eastern Mediterranean and the Levant: Tectonics of continental collision. *Tectonophysics*, Vol. 46, Pp. 297-311.
- Ritzmann, O., N. Maercklin, J. I. Faleide, H. Bungum, W. D. Mooney, and S. T. Detweiler, 2007.** A three-dimensional geophysical model of the crust in the Barents Sea region: model construction and basement characterization. *Geophysical Journal International*, 170 (1), 417-435, doi:10.1111/j.1365-246X.2007.03337.x.
- Robertson, A.H.F, Kidd, R.B., Ivanov, M.K., Limonov, A.F., Woodside, J. M., Galindo-Zaldivar, J., Nieto, L., 1995.** Eratosthenes Seamount: collisional processes in the easternmost Mediterranean in relation to the Plio-Quaternary uplift of southern Cyprus, *Terra Nova Volume 7, Issue 2*, pages 254–264, Article first published online: 1 JUL 2007, DOI: 10.1111/j.1365-3121.1995.tb00693.x
- Robertson, A.H.F., 1992.** Drilling the Eratosthenes Seamount: Mediterranean collision tectonics and Plio-Quaternary palaeo-oceanography in the light of the geology of Cyprus. *Rapp.Comm. Mer Medit.*, 33:393.
- Robertson, A.H.F., Dixon, J.E., 1984.** Introduction: aspects of the geological evolution of the Eastern Mediterranean. In: Dixon, J.E., Robertson, A.H.F. (Eds.), *Geological Evolution of the Eastern Mediterranean*. *Geol. Soc. Spec. Publ. London*, vol. 17, pp. 1–74.
- Ross, D. A. and E. Uchupi, 1977.** structure and sedimentary history of Southeastern Mediterranean Sea. Nile cone area, *AAPG bulletin* 61, N 6, pp. 892-902.
- Ryan, W.; Stanly, D.; Hersey, J.; Fahlquist, D. and Allan, T., 1971.** The tectonics and geology of the Mediterranean Sea. In: M. N. Hill (ED.), *The Sea*, Vol. 4, Part II, Wiley Interscience, New York, Pp. 387-492.
- Rybakov, M., Goldshmidt, V., Rotstein, Y., 1997.** New compilation of the gravity and magnetic maps of the Levant. *Geophys. Res. Lett.* 24, 33-36.
- Sage, L., Letouzey, J., 1990:** Convergence of the African and Eurasian Plate in the Eastern Mediterranean, *Petroleum and Tectonics in Mobile Belts*, Paris p. 49-68.
- Said, R., 1962.** The geology of Egypt. El sevier publishing co., Amsterdam, New York, P. 377.
- Schmidt, S. und Götze, H. J.,1998:** Program Documentation IGMAS. Institut fuer Geologie, Geophysik und Geoinformatik der FU Berlin, unveroeffentlicht. 41 Seiten.
- Segev, A and Rybakov, M, 2010.** Effects of Cretaceous plume and convergence, and Early Tertiary tectonomagmatic quiescence on the central and southern Levant continental margin, *Journal of the Geological Society of London*, v. 167 no. 4 p. 731-749, doi: 10.1144/0016-76492009-118
- Segev, A., M. Rybakov, V. Lyakhovsky, A. Hofstetter, G. Tibor, V. Goldshmidt, and Z. Ben Avraham, 2006.** The structure, isostasy and gravity field of the Levant continental margin and the southeast Mediterranean area, *Tectonophysics*, 425, 137–157, doi:10.1016/j.tecto.2006.07.010.
- Sengör, A.M.C., Gorur, N., Saroglu, F., 1985.** Strike-slip faulting and related basin formation in zones of tectonic escape: Turkey as a case example. In Biddle, K.T., Cristie-Blick, N., eds., *Strike-Slip Deformation, Basin Formation and Sedimentation*, Society of Economical Paleontologists and Mineralogists Special Publication, vol. 37, pp. 227-264.
- Smith, A.G., 1971.** Alpine deformation and the oceanic areas of the Tethys, Mediterranean and Atlantic: *Geol. Soc. Am. Bull.*, v. 82, p. 2039-2070.
- Smith, D.; Kolonkiewicz, R.; Robbins, J.; Dunn, P. and Torrence, M., 1994.** Horizontal crustal motion in the central and Eastern Mediterranean inferred from satellite laser ranging measurements. *Geophysical Research Letters*, Vol. 21, No. 18, Pp. 1979-1982.

- Stampfli, G.M., Borel, G.D., 2002.** A plate tectonic model for the Paleozoic and Mesozoic constrained by dynamic plate boundaries and restored synthetic ocean isochrons. *Earth Planet. Sci. Lett.* 196, 17–33.
- Ten Veen, J.H., Woodside, J.M., and Zitter, T.A.C., 2004.** The enigma of the Hellenic – Cyprus arcs' junction solved, in Chatzipetros, A.A., and Pavlides, S.B., eds., 5<sup>th</sup> International Symposium on Eastern Mediterranean Geology, Thessaloniki, Greece, vol. 1, pp. 201-204.
- Van der Meijde, M., S. van der Lee and D. Giardini, 2003.** Crustal structure beneath broadband seismic stations in the Mediterranean region, *Geophys. J. Int.*, 152, 729739.
- Vidal, N., Alvarez-Marrón, J., Klaeschen, D., 2000.** Internal configuration of the Levantine Basin from seismic reflection data (eastern Mediterranean), *EPSL*, Volume 180, Issues 1–2, [http://dx.doi.org/10.1016/S0012-821X\(00\)00146-1](http://dx.doi.org/10.1016/S0012-821X(00)00146-1)
- Woodside, J. M., 1977.** Tectonic elements and crust of the Eastern Mediterranean Sea. *Marine Geophys. Res.*, 3, 317-354.
- Woodside, J. and Bowin, C., 1970.** Gravity Anomalies and Inferred Crustal Structure in the Eastern Mediterranean Sea, *Geological Society of America Bulletin*, 81, 1107-1122.
- Woodside, J.M., 1976.** Regional vertical tectonics in the Eastern Mediterranean. *Geophys. J R Astron. Soc.*, 47: 493- 514.